EUROfusion

EUROFUSION WPPFC–PR(15)19

L. Gao et al.

Interaction of Deuterium Plasma with Sputter–Deposited Tungsten Nitride Films

Preprint of Paper to be submitted for publication in
Nuclear Fusion

This work has been carried out within the framework of the EUROfusion Consortium and has received funding from the Euratom research and training programme 2014-2018 under grant agreement No 633053. The views and opinions expressed herein do not necessarily reflect those of the European Commission.

"This document is intended for publication in the open literature. It is made available on the clear understanding that it may not be further circulated and extracts or references may not be published prior to publication of the original when applicable, or without the consent of the Publications Officer, EUROfusion Programme Management Unit, Culham Science Centre, Abingdon, Oxon, OX14 3DB, UK or e-mail Publications.Officer@euro-fusion.org".

"Enquiries about Copyright and reproduction should be addressed to the Publications Officer, EUROfusion Programme Management Unit, Culham Science Centre, Abingdon, Oxon, OX14 3DB, UK or e-mail Publications.Officer@euro-fusion.org".

The contents of this preprint and all other EUROfusion Preprints, Reports and Conference Papers are available to view online free at http://www.euro-fusionscipub.org. This site has full search facilities and e-mail alert options. In the JET specific papers the diagrams contained within the PDFs on this site are hyperlinked.

Interaction of Deuterium Plasma with Sputter-deposited Tungsten Nitride Films

L. Gao[1, 2], W. Jacob[*1], G. Meisl[1], T. Schwarz-Selinger[1], T. Höschen[1], U. von Toussaint[1] and T. Dürbeck[1]

1. Max-Planck-Institut für Plasmaphysik, Boltzmannstr. 2, 85748 Garching, Germany

2. Institute of Plasma Physics, Chinese Academy of Sciences, Shushanhu Rd. 350, 230031 Hefei, China

Abstract

Magnetron-sputtered tungsten nitride (WN_x) films were used as a model system to study the behavior of re-deposited WN_x layers which could form in fusion devices with tungsten (W) wall during nitrogen seeding. The interaction of such WN_x layers with deuterium (D) plasmas was investigated in dedicated laboratory experiments. D retention and N removal due to D plasma exposure at different temperatures were measured with ion beam analysis (IBA). Low-energy argon sputtering followed by IBA was applied to resolve the D distribution in the top-most surface of WN_x with significantly improved depth resolution compared with the standard D depth profiling method by nuclear reaction analysis. Experimentally determined thicknesses for the penetration of D in WN_x were compared with the penetration depth for D calculated in SDTrimSP simulations. Results show that D is only retained within the ion penetration range for samples exposed at 300 K. In contrast to the 300 K case, D diffuses beyond the implantation depth in a sample exposed at 600 K. However, the D penetration depth is much lower than in pure W at comparable conditions. The total amount of retained D in WN_x at 600 K is by 50% lower than for implantation at 300 K with the same D fluence. Nitrogen is removed only within the D ion range.

Key words: Plasma wall interaction; Tungsten; Nitrogen seeding; Tungsten nitride; Deuterium retention; Deuterium-rich surface layer.

PACS: 28.52.Fa , 52.40.Hf, 79.20.Rf, 52.77.Bn

[*] Corresponding author. Fax: +49-3299-1504, Tel: +49-3299-2618.

E-mail address: wolfgang.jacob@ipp.mpg.de

1. Introduction

Interaction of the boundary plasma with the plasma-facing surfaces will lead to re-deposition of wall materials and fuel retention in the plasma-facing components. Retention of hydrogen isotopes, especially in next generation fusion devices where a mixture of deuterium (D) and tritium (T) will be used as fuel, is of great importance due to safety and cost concerns [1]. For fusion devices with all metal walls, such as ASDEX Upgrade and JET, impurity seeding is necessary for radiative power dissipation to reduce the peak power load onto the divertor [2, 3]. Recent experiments in ASDEX Upgrade using a full-W first wall [4-6] and JET with the ITER-like Wall [7, 8 and references therein] had shown that nitrogen has favorable properties in cooling the edge plasma and enhancing plasma performance. The presence of N_2 as a new plasma species will lead to additional plasma-surface interactions such as implantation, retention, sputtering and possibly co-deposition together with sputtered W. Co-deposited WN_x layers were already observed in TEXTOR after N_2-seeded discharges [9]. So far there are only very few reports on the interaction of D plasma with co-deposited WN_x layers in fusion devices during or after nitrogen seeding. For a reliable assessment of the plasma-surface-interaction behavior and the hydrogen-isotope inventory in nitrogen containing W, it is mandatory to investigate the retention and diffusion of D in such WN_x layers. Furthermore, the erosion behavior of these co-deposited layers by D plasma is of great importance for understanding the plasma-surface-interaction in N_2-seeded plasmas.

Recent experiments [10, 11] have indicated that the formation of WN_x or the presence of a N-containing layer formed by N implantation reduces reemission of D through the surface thus leading to increased D retention at elevated temperature. In our preceding study [12], sputter-deposited WN_x films deposited on bulk W substrates were exposed to D plasma at 300 K for studying the behavior of co-deposited WN_x layers in fusion devices during or after discharges with N_2 seeding. Results showed that D implanted at 300 K into WN_x films is retained only in a very thin layer with a thickness comparable to the ion penetration range of the impinging D ions and does not, as in bulk W, diffuse to larger depth. In the present work, we extend this study to higher temperature (600 K) and make comparison with 300-K exposures. Low-energy argon sputtering combined with ex-situ ion beam analysis (IBA) [12] after D exposure was applied to determine the D depth profiles in the top-most surface. Additional attention was paid on the erosion of the WN_x films by D plasma using both IBA and XPS measurements. Furthermore, the thermal release behavior of N and D from WN_x films was investigated by temperature programmed desorption (TPD). Based on this, the D retention and its diffusion behavior in sputter-deposited WN_x layers exposed to low-flux D plasma will be discussed. Finally, the N removal was measured as a function of D fluence which is expected to be helpful for understanding N migration in edge plasmas.

2. *Experimental details*

2.1 Sample preparation

Single crystal (100) silicon wafers were cut into pieces with area of 10×10 mm^2 as substrates for film deposition. All the Si pieces were then ultrasonically cleaned in propanol and acetone. A W film was deposited as an interlayer before and WN_x films were grown onto these Si substrates. There are two reasons why WN_x films were not directly deposited onto Si substrates. First, since samples shall later be exposed at elevated temperature, a W film as interlayer will avoid the possible interaction of N with Si during heat treatment. Second, Si shows similar to N also a nuclear reaction with ^4He and the proton spectra from N and Si overlap [13]. The silicon signal can be suppressed when the W interlayer is thicker than ~2 μm.

The depositions were performed using a commercial sputtering device (Discovery®18, Denton). The system was pumped down to a base pressure of less than 5×10^{-5} Pa. A liquid N_2 cold trap was used to reduce the water partial pressure. Prior to deposition the Si substrates were etched with argon for 2 min (0.5 Pa Ar). The applied RF power of 100 W resulted in a substrate bias voltage of -580 V for surface etching. W film deposition was performed in an atmosphere of 0.7 Pa Ar for 120 min. With an applied DC power of 300 W a cathode bias of -380 V was generated. According to our previous results [14, 15], the deposition rate of W film under these conditions is about 18.5 nm/min. Therefore, 120 min deposition will give rise to a 2.2 μm thick W film. WN_x layers (0.6 Pa, 50% Ar, 50% N_2, 300 W RF power resulting in -370 V cathode bias) were in the following deposited on top of the W films for 5 and 15 min, respectively. To ensure a homogeneous thickness for all the samples, the substrate holder was rotating through the whole deposition process. In order to avoid a possible contamination of the W surface, the WN_x layers were deposited immediately after W film deposition without breaking the vacuum. One of the Si substrates was partially covered by adhesive Kapton tape. Removing the tape after deposition produced a step which allowed measuring the thickness of the complete deposited layer system by tactile profilometry. The full layer system with 15 min WN_x deposition was about 2.35 μm thick which indicated that the thicker WN_x layers were about 150 nm thick. The precise thickness of the WN_x layer was determined from a cross-section image. From the cross section produced in a scanning electron microscope equipped with a focused-ion-beam the layer thicknesses were measured to be 135±5 nm for the thicker samples and 45±5 nm for 5-min-deposited samples. One set of thicker samples and one thinner sample were annealed in vacuum at a temperature of 600 K for 2 hours. The annealed thicker samples were later exposed to D plasma at 300 K together with the as-deposited layers. This was done to allow distinguishing the effect of exposure temperature on D retention from possible annealing-induced

structural changes within the sputter-deposited WN_x films at 600K. The annealed thinner sample was used for thermal decomposition measurements (see next section). This thin film is assumed to show the same thermal behavior as the 135 nm thick films.

2.2 *Thermal stability of WN_x layer*

Since some of the deposited WN_x layers were exposed to D plasma at 600K, it was necessary to study the thermal stability of the present WN_x films, i.e., to determine at which temperature the used WN_x layers start to decompose. For this, temperature programmed desorption (TPD) was used. TPD measurements were performed in the quartz tube of the TESS device [16]. The temperature response of the samples to the linear oven temperature ramp was calibrated in independent experiments by a thermocouple connected to a Si wafer of identical size. The samples were heated with an oven heating rate of 15 K/min up to a sample temperature of 1273 K, which is expected to be high enough to ensure desorption of all N from the layers.

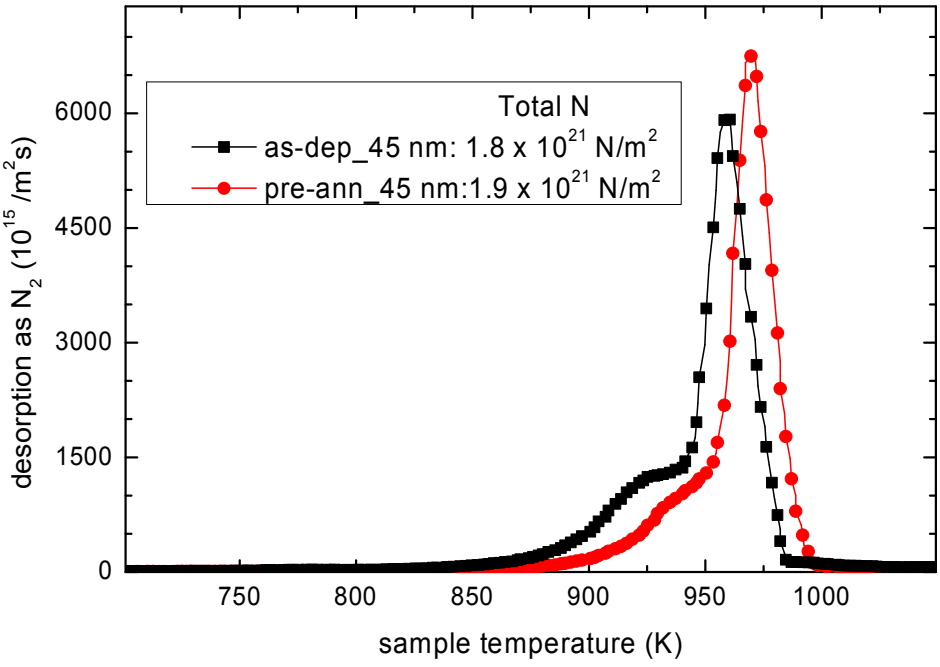

Fig.1 TPD spectra on N_2 release from a 45 nm thick magnetron-sputtered WN_x films deposited on 2-µm-W-coated-Si substrates.

The desorbed gases were measured with a quadrupole mass spectrometer (QMS). The secondary electron multiplier of the QMS was operated in single ion counting mode to minimize the background noise and to be able to apply Poisson statistics for determining the accuracy. The following 8 masses were recorded as a function of time: 12, 14, 16, 20, 28, 32, 40, and 44 amu/q. For the quantitative analysis the QMS signals for N_2 was calibrated with pure N_2 gas. For this purpose a constant gas flow was introduced into the UHV chamber through a calibrated orifice and the QMS signal was measured. With the orifice size and the upstream pressure measured with a spinning rotor gauge a calibration factor for N_2 of 3.8×10^9 N_2 molecules per count was deduced. The experimental uncertainty was determined by consecutive calibration measurements and was governed by the stability of the detector rather than by determination of the flow. As a result, the inaccuracy of the present TPD measurement for quantification of N is better than 10%.

Thinner WN_x layers (about 45 nm) on top of W-coated Si substrates were used for TPD measurements. The TPD spectra of the as-deposited and the WN_x layer annealed for 2 h at 600 K are shown in Fig. 1. Decomposition of both as-deposited and annealed WN_x layers starts at around 830 K. The release spectra are composed of two release peaks. The first one is a shoulder at lower temperature followed by the main peak. The height of the shoulder is about 20 % of the main peak. The peak positions for the as-deposited WN_x layer are 925 and 960 K and for the WN_x layer previously 940 and 970 K. The integral of the release peaks over time, which is directly proportional to the total released N_2 amount (as stated in the figure), is identical within the experimental uncertainty for both layers. The shift of the release spectrum of the pre-annealed layer to higher temperatures is presently unexplained. It might be explained by a transformation to a slightly more stable phase during annealing. Actually, X-ray diffraction measurements on thick WNx layers (2 μm) grown in the same way before and after annealing at 600 K for 2 hours showed no measurable difference on the acquired diffraction pattern. But, of relevance for the present investigation is the fact that N_2 release starts only at temperatures of about 830 K which is much higher than the annealing and the selected D implantation temperatures of 600 K. In addition, the fact that the peak integrals of the as-deposited and of the annealed layers are identical clearly shows that during the 2 h annealing at 600 K no measurable loss of nitrogen from the layer occurs. Therefore this shift is of no relevance for the present investigation. Assuming that the WN_x films deposited onto the side faces of the Si substrate increase the total WN_x-covered area by about 15 % compared with the top surface area only, the N amount measured by TPD is in good agreement with the nitrogen amount determined by ion beam analysis presented further below. Unfortunately it was not possible to check if there was still N remaining in the layer after TPD measurements, because all the

deposited layers delaminated from the substrate due to the largely different thermal expansion compared to the Si substrates.

2.3 D implantation

D implantation was performed in the low-pressure electron cyclotron resonance (ECR) plasma chamber 'PlaQ'. PlaQ was described before and the details can be found in Ref. [17]. At the used pressure of 1.0 Pa the D plasma delivers predominantly D_3^+ ions (94 %) with minor contributions of D_2^+ (3 %) and D^+ (3 %) [17]. D plasma was burned-in for 15 min without exposing the sample to the plasma beam by closing the shutter between the aperture and the sample holder. A DC bias voltage was applied to the substrate holder once the shutter was opened. The -200 V DC bias voltage together with the plasma potential of about -15 eV [17] resulted in an ion energy of 215 eV. For the dominant ion species D_3^+ this corresponds to an energy of 72 eV per deuteron and correspondingly to 108 eV per D for the D_2^+ ions and 215 eV per D for the D^+ ions. The total D flux was 9.9×10^{19} D·m^{-2}s^{-1}. D plasma exposures with fluences ranging from 1.0×10^{23} D/m^2 to 6.0×10^{24} D/m^2 were performed for the three different sets of samples at two different sample temperatures. Namely as-deposited samples were exposed at 300 K and 600 K, and 600 K pre-annealed samples at 300 K. The samples were mounted with screws at tungsten coated copper (temperature range: 230-450 K) or stainless steel (450-800 K) holder. The rise of the temperature at the sample surfaces due to the ion bombardment was monitored by an infrared camera. The sample temperature was controlled by keeping the cooled holder at ~295 K with a thermostat circuit of ethanol cooling and with radiative heating at ~575 K for the heated holder, respectively. By this, the temperature at the sample surface was stabilized at 300 respectively 600 K. Note that the D implantations at 600 K were not performed for pre-annealed samples, since a comparable annealing effect will occur during heating of the samples to steady state temperature prior to starting the D plasma exposure anyway. Also, the radiative heating was switched off 2 min before ending the implantation with the set D fluence. The cooling of the heated holder was performed by keeping a pressure of 500 Pa in the chamber with D_2 atmosphere.

2.4 X-ray photoelectron Spectroscopy (XPS)

X-ray photoelectron spectroscopy (XPS) measurements were performed using a Perkin Elmer PHI 5600 ESCA system with a hemispherical analyzer. The standard X-ray source was used to record spectra with Mg-Kα radiation (1253.6 eV). The Omni focus lens restricted the analyzed area to a spot with a diameter of 400 µm. The analyzer was operated at constant pass energy of 5.85 eV. Energy calibration for

all the measurements were performed using pure Au, Ag and Cu samples and a precision of 0.1 eV was confirmed. For depth profiling an 10 kV Ar^+ ion beam was scanned over an area of 1500×1200 μm^2. The angle of incidence for the Ar^+ ion beam was 20° to the surface normal. For evaluation of the measured XPS spectra a Shirley background function was applied for background subtraction. Standard relative sensitivity factors supplied by the manufacturer were used to estimate atomic concentrations.

2.5 Ion Beam Analysis

To investigate the D retention in the sample and the erosion of WN_x, the samples were before and after plasma exposure characterized by ion beam analysis. Nuclear reaction analysis (NRA) was applied for measuring the retained D amount with D (^{3}He, p) ^{4}He nuclear reaction and ^{4}He Rutherford backscattering spectroscopy (RBS) was used for determining the erosion of WN_x films. The produced high energy protons from NRA were counted using a thick, large angle solid state detector at a scattering angle of 135° equipped with a curved slit reducing the solid angle to 29.9 msr. In the experiments presented here a $^3He^+$ ion beam with an energy of 500 keV was used to determine the near surface D distribution by NRA. We define the information depth for the NRA analysis as the depth where the kinetic energy of the projectiles decreased to about 420 keV (the energy where the cross-section is 10% as the maximum value at 620 keV [18]) for the here applied nuclear reaction. This information depth was calculated applying SIMNRA [19] with Ziegler/Biersack stopping power data. The generated protons have a very high energy of about 13.5 MeV. The mean free path of these high energy protons is much larger than this information depth, such that the generated protons can easily reach the detector. At 500 keV, the NRA information depth in WN_x is 680 nm for the high energy protons. For the given experimental geometry, the corresponding depth resolution from protons at the surface is 110 nm according to RESOLNRA [19]. For the produced α particles, the depth resolution is better due to the much stronger stopping by the material than for the high-energy protons. For our experimental setup the best achievable resolution for α particles at 500 keV projectile energy is roughly 16 nm. For the method presented here only the proton signal was evaluated because it provides a four times higher count rate for our experimental setup. The D amount in the sample was quantified using the cross section published by Alimov et al. [18]. For comparison and reference an about 10 nm thick plasma-deposited amorphous deuterated carbon film (a-C:D) on a Si wafer with a D amount of 6.7×10^{20} D atoms/m^2 was also measured by the same ^{3}He ion beam. The NRA information depth in a-C:D is larger than the above stated values for WN_x so that the full a-C:D layer contributes to the NRA proton signal.

The erosion of the WN_x layers was measured by RBS using 1.5 MeV $^4He^+$ projectiles. The backscattered ^{4}He particles were counted with a detector at a scattering angle of 165° with a solid angle of 1.10 msr.

The measured RBS spectra were simulated with SIMNRA [19] using Ziegler/Biersack stopping power data and taking dual scattering into account. Based on this simulation the N amount before and after D implantation and the removed layer thickness due to D plasma exposure were determined.

2.6 Low-energy Ar sputtering for D depth profiling

In a recent publication we have shown that the resolution for D depth profiling can be significantly improved compared to standard NRA by consecutive low-energy argon plasma sputtering followed by ion beam analysis [12]. For this reason, low-energy Ar plasma sputtering was also performed in PlaQ for samples exposed to a D fluence of 1.0×10^{24} D/m^2 from the aforesaid three groups. The Ar pressure was 0.25 Pa and the applied DC bias voltage -200 V. To reduce the implantation of impurities from the Ar plasma due to venting, 15-min plasma burn-in was also performed until the chamber cleaned itself. Before applying the DC bias, all samples were exposed to Ar plasma at floating potential (3 V) for 10 min to gently remove adsorbed impurities. To reduce a possible D loss during sputtering the sample temperature was kept at 230 K using the ethanol cooling circuit. To ensure a thorough comparison of D retention and a detailed reconstruction of the D depth profiles, different durations of Ar-plasma exposure on different sections of the identical sample were performed by partially covering the sample surface with a 50 micron thick W foil while keeping other parts exposed to Ar plasma. Because the sputtering experiments on different areas of the sample cannot be performed within one Ar plasma exposure, the chamber had to be opened for rearranging the tungsten-foil cover several times. For example, to produce four sectors on one sample with Ar exposure times of 5, 10, 20 and 25 min we first covered one half of a D-implanted sample with the tungsten foil and exposed the uncovered half to Ar plasma for 15 min. Then for the second Ar plasma exposure we rotated the foil by 90 degrees thus covering the perpendicular half of the sample. That means one quarter of the sample that was previously covered and another quarter that was previously sputtered for 15 min were exposed in the second, 5 min long Ar plasma exposure thus producing areas that in total experienced Ar sputtering for 5 and 20 min. In the final step this sample was exposed to Ar plasma without W-foil cover for additional 5 min such that this sample had four different quarters which were exposed to Ar plasma for 5, 10, 20 and 25 min. Another identical sample was exposed similarly as the first sample, but with 15 min intervals thus producing a sample with 0, 15, 30, and 45 min Ar plasma exposure. Finally, 8 areas with different Ar sputtering durations were produced on 2 identical samples, namely 7 areas from 0 to 30 min with 5 min sputtering intervals and additionally one area with 45 min Ar sputtering.

After low-energy Ar sputtering of different durations the corresponding sections of the sample surfaces were further characterized by NRA and RBS for the remaining D amount and WN_x layer

thickness, respectively. Based on this, the amount of sputtered WNx layer and the removed D amount can be determined. Combining the experimental results from RBS and NRA, the depth distributions of D in the top-most surface were reconstructed with a resolution of ~3 nm which is more than 5 times better than the resolution obtained by analyzing the alpha signal.

2.7 Thermal release of D from WN_x by TPD

After the NRA measurements the released D amounts of several selected samples were measured by TPD in TESS (see Sect. 2.2). Additional mass channels were traced in these experiments. Besides mass channels 2 (H_2), 3 (HD) and 4 (D_2), mass channels 18 (NH_2D), 19 (NHD_2) and 20 (ND_3) were also included to monitor the possible release of deuterated ammonia. The calibration for D_2 and HD was done similarly as for N_2 and the determined calibration factors were 4.1×10^8 D_2- and 4.2×10^8 HD-molecules per count, respectively. The calibration of deuterated ammonia, however, was not possible. On the one hand, ammonia sticks strongly to the chamber wall such that the introduction of large amounts of ammonia for calibration would pollute the whole TESS device. On the other hand, the same mass of different deuterated ammonia and water isotopologues (18 amu for both NH_2D and H_2O, 19 amu for NHD_2 and HDO and 20 amu for ND_3 and D_2O) cannot be distinguished with a standard low-mass-resolution QMS. Hence, the total amount of D released in form of hydrogen molecules was calculated from the integral of the D_2 (4 amu) and HD (3 amu) peaks. It has to be stressed that this is only a lower limit to the retained D amount in the samples for two reasons: Firstly, some of the D in the layers is released in form of water and ammonia which cannot be quantified as discussed above, Secondly, because the layers completely delaminated from the substrate because of the TPD analysis we could not check whether some D still remains in the layers.

3. Characterization of the WN_x layer

WN_x layers were characterized with RBS for the initial areal density as well as the N amount and concentration. Fig. 2a shows a full RBS spectrum (measured with 1500 keV $^4He^+$) of as-deposited WN_x layer sample exposed to D fluence of 1.0×10^{24} D/m^2 prior to Ar sputtering. For comparison the simulated RBS spectrum of a W film without WN_x coating is also shown as a dashed line in the figure. The measured data is represented by symbol and the corresponding SIMNRA [19] simulation by solid line. The simulated spectrum does not fit very well to the experimental data at low backscattering energy. This can be explained by the large uncertainty of the stopping power and cross-section data at low projectile energies. However, in the relevant energy range ($E > 1000$ keV) the simulated spectrum fits the experimental data very well. The relevant information from the near surface region appears in the backscatter energy range from about 1200 to 1400 keV. This region is enlarged as the inset of Fig. 2a.

The W concentration within the coating – corresponding to the RBS signal from the high energy edge at about 1370 keV to the interface to the pure W layer located at about 1220 keV – is lower than for the W substrate because of the presence of nitrogen. The step located at about 1220 keV marks the transition from the WN_x layer to the underlying W film. Without WN_x coating, as shown by the spectrum of pure W no such step appears. The width of the W-depleted region in the RBS spectra corresponds to the areal density of the WN_x layer and the height of the RBS signal at a specific energy depends on the local W concentration. The RBS signal of the N species in the WN_x layer, which should appear in the backscattering energy range of 350-480 keV, cannot be directly seen due to the intense W signal and the low cross section for N. However, the N concentration in the WN_x layers can be derived from a simulation of high energy part of the RBS spectrum by SIMNRA [19]. Adding nitrogen to the W-depleted zone within SIMNRA one can fit the experimental curve. The assumption that N is the only species that dilutes W in this layer is valid as the oxygen and carbon content is less than 1 % as measured with XPS.

As a result of that fitting procedure a W concentration in the WN_x layer of (56±2) % is deduced. The measured areal density of the as-deposited layer before D implantation is 1.0×10^{22} atoms/m^2 and after D exposure with fluence of 1.0×10^{24} D/m^2 it is 9.4×10^{21} atoms/m^2. Obviously, 6.0×10^{20} atoms/m^2 WN_x layer had been removed by the D implantation. Together with the initial thickness measurement of the deposited film (135±5 nm, see Sect. 2.1), we can determine the atom number density of our WN_x layer. It is roughly 7.4×10^{28} atoms/m^3. Based on this density, we can calculate from the RBS data the removed layer thicknesses by each sputtering step for later used D depth profiling.

4. D retention in WN_x

4.1 D depth profiles

As mentioned above, D plasma exposure of WN_x layers was performed for three different cases: a) as-deposited layers exposed at 300 K, b) as-deposited layers exposed at 600 K and c) layers annealed prior to exposure for 2 h at 600 K and then exposed at 300 K. From each of these cases, the sample that was exposed to a D fluence of 1.0×10^{24} D/m^2 was selected for low-energy Ar sputtering for D depth profiling (see Sect. 2.5). Samples with WN_x coatings after different Ar sputtering times are presented in Figs. 2b to d. Note that, only the interesting near surface regions (1200-1400 keV) were shown. As anticipated, the area without Ar sputtering shows always the thickest WN_x layer. With increasing sputtering time the edge of the pure W interlayer shifts to higher backscattering energies indicating the decrease of the thickness of the WN_x layer on top. For clarity, only selected RBS spectra are shown in Figs. 2b-d, because a 5-min Ar sputtering step removes only a very small amount of WN_x. One RBS

spectrum shown in Fig. 2c stems from an area after 180-min Ar sputtering. In this case the shift of the pure-W edge is most pronounced and the thickness of the remaining WN_x layer is only about 40 nm. The amount of sputtered WN_x was determined by fitting the RBS spectra with SIMNRA assuming constant N concentration throughout the WNx films (no W enrichment within the Ar ion range). The RBS spectra in Figs. 2b and d look very similar to each other. This indicates that the pre-annealing had little or no influence on the layer stoichiometry and on the sputtering yield of these WN_x films. Each 5-min Ar sputtering interval removes about 2.7 nm WN_x layer for both as-deposited and pre-annealed samples. However, for the samples exposed at 600 K (Fig. 2c) each 5 min Ar sputtering interval removes only about 2.0 nm in average.

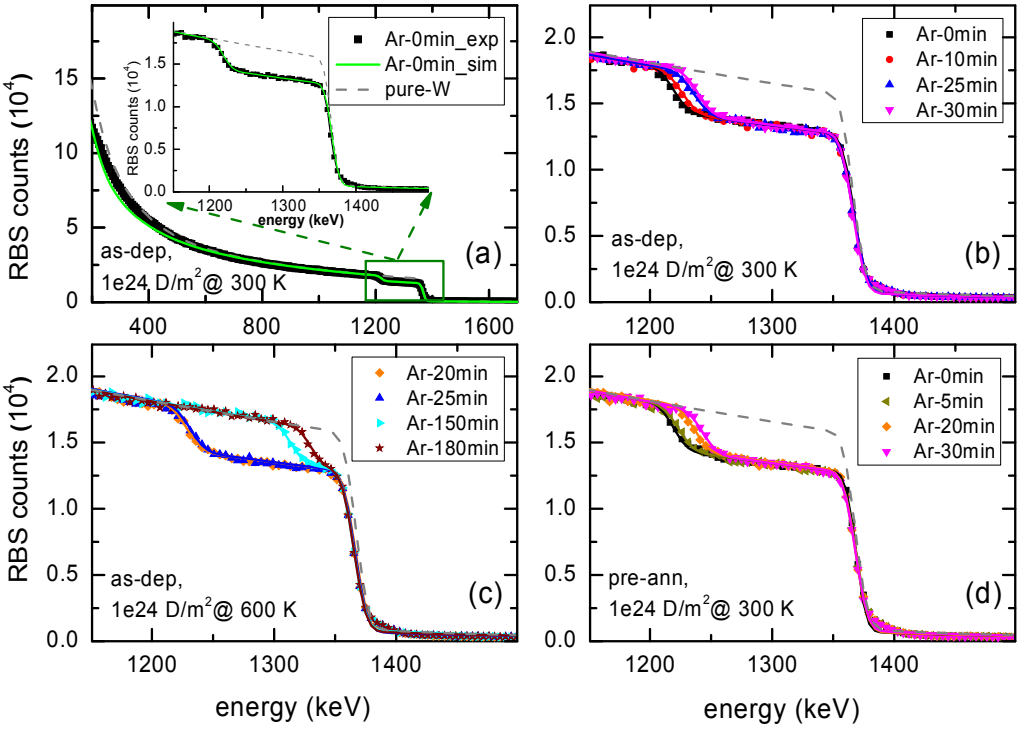

Fig. 2: RBS spectra of magnetron-sputtered WN_x films (deposited on Si substrates pre-coated with a 2 µm thick W film) after D plasma exposure at 300 and 600 K and after different Ar sputtering times (sputtering times are indicated in the figure): a) full RBS spectrum of an as-deposited sample exposed to D plasma at 300 K; b) enlarged view of the informational part (as indicated by the dashed box in (a)) from as-deposited samples exposed at 300 K; c) as-deposited samples exposed at 600 K; d) samples annealed for 2 h at 600 K and exposed at 300 K. In all subfigures symbols represent experimental data and solid lines SIMNRA simulation results (for details see text).

Fig. 3 shows the proton spectra from the nuclear reaction of D (^{3}He, p) α with a 500 keV $^3He^+$ ion beam after different Ar sputtering durations. In general, the proton yields, corresponding to the D amount remaining in the WN_x layer, decreases with the increasing Ar sputtering time. For both as-deposited (Fig. 3a) and pre-annealed (Fig. 3b) samples exposed to D plasma at 300 K 30 min Ar plasma sputtering is sufficient to almost completely remove the D-containing layer indicated by the disappearance of the proton signal. The sample exposed at 600 K differs in two regards: First, the initial proton signal is only about half of that as for 300 K exposure and, second, it takes much longer to remove the D-containing layer. It turned out that the proton peak disappeared only after 180 min Ar sputtering. However, the 5-min-Ar sputtered area of the pre-annealed sample (Fig. 3b) shows surprisingly a larger proton peak than that from the area without Ar sputtering. The reason for this deviation is unclear. Most probably it is due to an experimental outlier because the proton peak integral of the pre-annealed sample is also lower than for the as-deposited sample while all other proton spectra for these two samples agree. In any case, other data points show the expected decreasing behavior. Although this ambiguity is unsatisfactory it has no influence on the further evaluation of the data. According to the thickness calculation based on the RBS-determined atom density of our layers as discussed above, after 30 min Ar sputtering of the 300 K exposed sample about 16 nm WN_x is removed and 180 min sputtering of the 600 K exposed sample corresponds to about 100 nm. In all shown cases, the D-containing layers are much thinner than the information depth of the applied NRA measurements with a 500 keV projectile energy (~680 nm, see Sect. 2.5). From the disappearance of the proton peaks we conclude that for the here used D fluence of 1.0×10^{24} D/m^2 all D was retained in WN_x layer thicknesses of 16 nm for 300 K exposed samples and ~100 nm for samples exposed at 600 K.

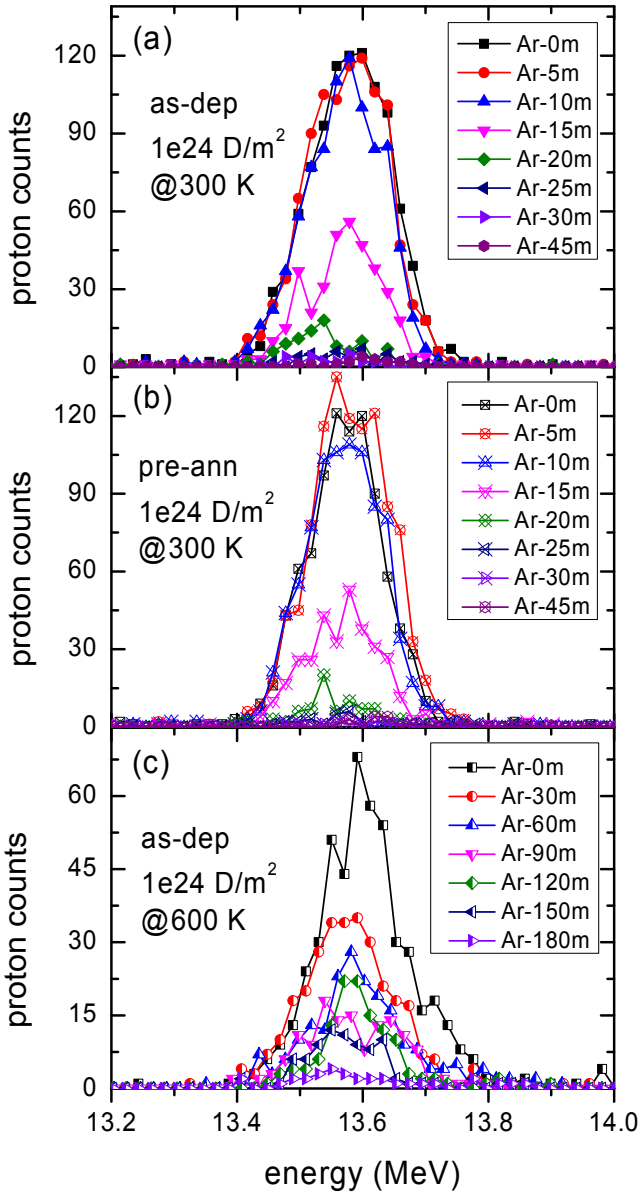

Fig. 3: NRA proton peaks of samples from Fig 2.

Based on the experimentally measured cross-section data from Alimov [19], the amounts of retained D in the remaining WN_x layers after each Ar sputtering step are calculated. The total D amounts determined from the proton signals are shown in Fig. 4 as a function of the removed WN_x layer thickness. The removed amount of WN_x layer is shown in units of atom areal density in the bottom x-scale and in 'nm' in the top x-scale of Fig. 4. The thickness scale is only indicative and was calculated using the

determined atom density as discussed further above. The total D amounts remaining in the WN_x layers exposed at 300 K decrease very fast with Ar sputtering time. For exposure at 300 K all D in the sample was retained in this 16-nm-thick WN layer. The non-linear decrease is most probably a consequence of an inhomogeneous D depth distribution. For the sample exposed at 600 K, the initially retained D amount before Ar sputtering is half of that at 300 K and the decreases with increasing Ar sputtering time is significantly slower than that at 300 K. Due to the lower total retained D amount and its larger penetration depth the local D concentration at 600 K is much lower than at 300 K.

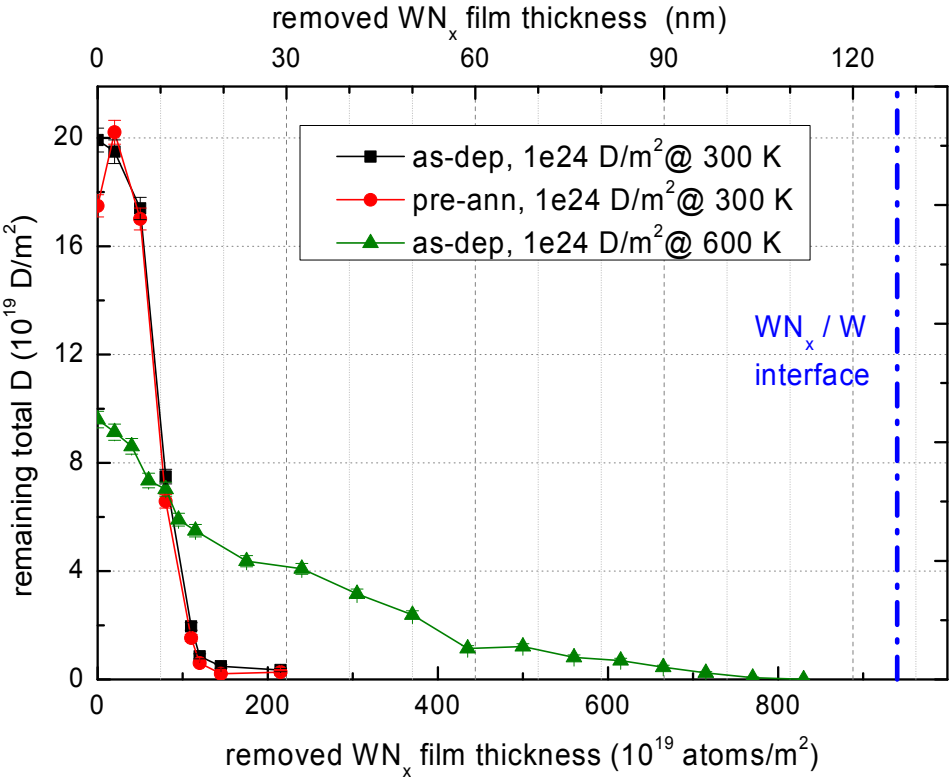

Fig. 4: Total D amount in WN_x samples exposed to 1×10^{24} D/m² at -200 V bias after different Ar plasma exposure durations. The lower scale shows the removed WN_x layer thickness in units of atoms/m²; the initial film thickness is about 9.4×10^{21} atoms/m². The upper scale is a thickness scale in nanometers calculated using a WN density of 7.4×10^{28} atoms/m³. The approximate position of the WN_x/W interface is also indicated.

On the basis of the total D amount remaining after sputtering as presented in Fig. 4 and the removed WN_x layer measured by RBS (Fig. 2) the D depth profiles in the WN_x layer can be determined. Thereby we assume that D is distributed uniformly within the removed WN_x layer from each sputtering step. The resulting D depth profiles of as-deposited samples exposed at 300 K and 600 K are shown in Fig. 5. The

depth profile for the pre-annealed sample is not plotted because it is almost identical to that of the as-deposited sample.

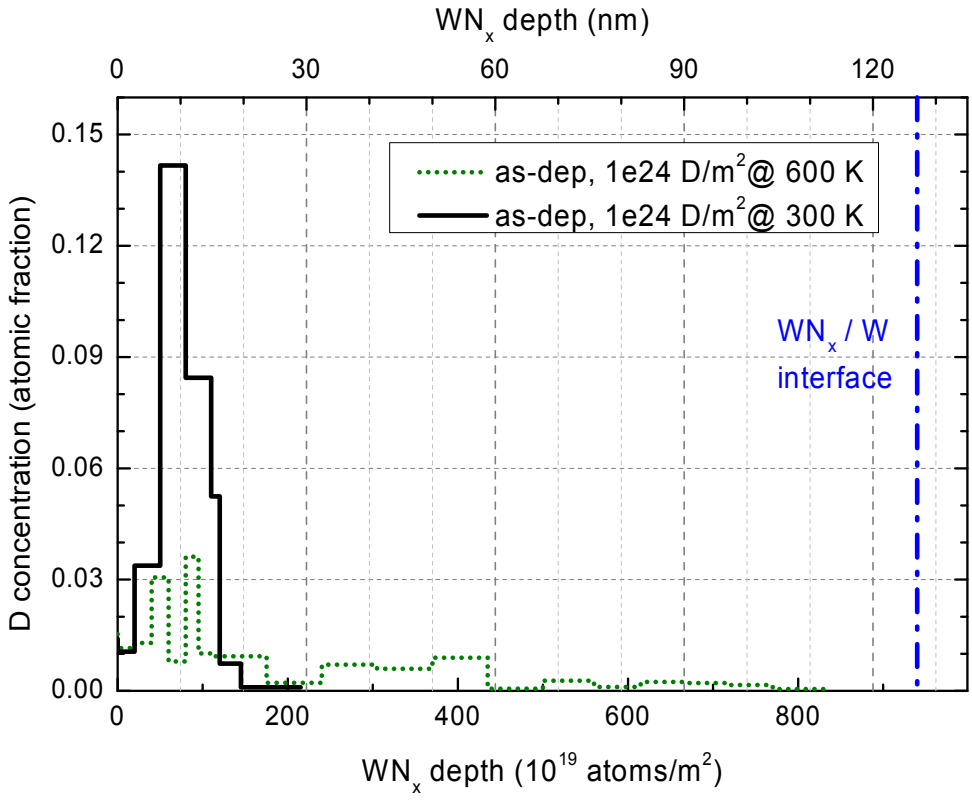

Fig. 5: Experimentally measured D depth profiles in WN_x samples after 1×10^{24} D/m^2 implantation. Note that the lower and upper x-scales are shown in different units. The upper scale is a thickness scale in nanometers calculated using a WN density of 7.4×10^{28} $atoms/m^3$.

As one can see in Fig. 5, at 300 K, the D in the WN_x layer first increases with increasing depth and reaches its peak concentration of about 14 at. % within a depth of 7-11 nm and then drops quickly to 1 at. % at ~16 nm. At larger depth, the D concentration is below 1 at. % and no D is detected beyond a depth of 20 nm. For D implantation at 600 K, the peak concentration is only about 3 at. % in a depth up to 14 nm, which is a factor of 5 lower than that of the 300 K-implanted samples. However, the D concentration remains at a level of a few atomic percent up to depth of ~60 nm. For larger depth the D concentration further decreases and no D is detected for a depth larger than 110 nm.

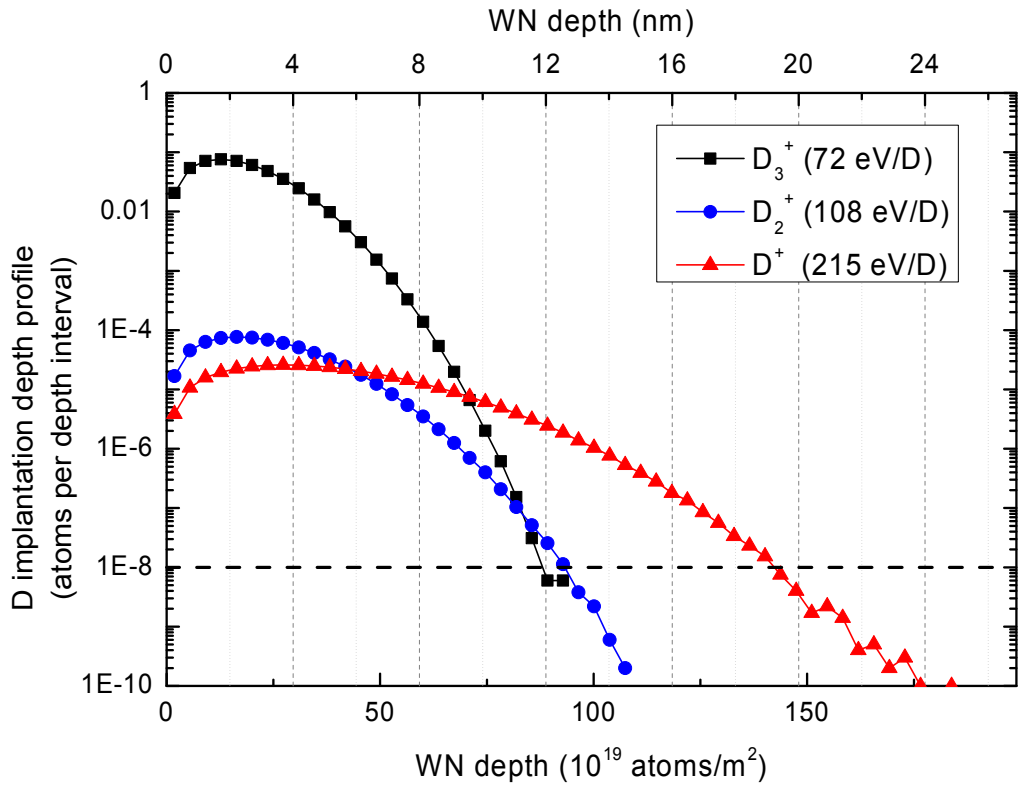

Fig. 6: SDTrimSP simulation of the distribution of implanted deuterons in WN matrix. Plotted is the probability to find an impinging deuteron in the given depth in a depth interval of 0.4 nm. The total incident amount of D is 10^9. The reflection coefficient is roughly 0.5 (for details see text). The lower x-scale shows the layer thickness in units of areal density (atoms per m^2); the upper x-axis shows a thickness scale in nanometers calculated using a WN density of 7.4×10^{28} atoms/m^3.

SDTrimSP [20, 21] simulations of D implantation were performed to interpret the present experimental results. The same W:N ratio as determined by RBS for our deposited layers was set as target matrix in the simulation. In total 10^9 projectiles were simulated, the cutoff energy of the projectiles was set to 2 eV and the target was discretized into layers with 0.4 nm thickness. The simulations were performed for normal impact angle and an energy distribution corresponding to a D flux consisting predominantly from D_3^+ ions (94%) and minority contributions of D^+ (3%) and D_2^+ ions (3%). The molecular ions are treated as individual deuterons impinging with the same velocity. For example, a D_3^+ ion with energy of 215 eV, as in the present case, will be treated as three impinging deuterons with energy of 72 eV and a D_2^+ corresponds to two deuterons with energy of 108 eV. The simulated D implantation depth distributions for the fixed ion energy of 215 eV resulting in three different energies per deuteron as just explained are plotted in Fig. 6. The simulations were performed in static mode, that means the

possible retention of D in the matrix as well as preferential erosion of N from the matrix were not taken into account, or with other words each D impinged on the pure, D-free W:N matrix.

Before interpreting the simulation results it is advisable to recall what SDTrimSP can simulate and what not. TRIM and related simulation tools describe the transport of energetic ions in matter on the basis of the binary collision approximation. In our case, the results presented in Fig. 6 describe how far an energetic particle penetrates into the matrix material before its kinetic energy drops below 2 eV. SDTrimSP cannot describe what happens with the particle after it has lost its kinetic energy. In particular, it cannot describe the possible diffusion of a thermalized species. That means Fig. 6 shows the penetration probability distribution (range distribution) of the D species mix according to the species composition of our plasma impinging on a WN_x layer. The deuterons impinging in form of D_3^+ ions are shown by the diamonds in Fig. 6. Since their contribution to the total flux is highest the probability to find them in the layer is also largest. But with the lowest energy per deuteron, their penetration depth is also smallest. The deuterons impinging in form of D_2^+ ions (circles) have a somewhat higher energy and a much lower intensity. Due to the slightly higher energy than the deuterons impinging in form of D_3^+ they penetrate slightly deeper. Finally, deuterons impinging as atomic ions (triangles) have an even lower probability but a significantly higher penetration depth. If we take quite arbitrarily a level of 10^{-8} in Fig. 6 as cutoff the penetration depths for the three different ion species are about 12, 13 and 19 nm, respectively. In addition to penetration SDTrimSP also yields the reflection coefficient. The reflection coefficients for the three different energies per deuteron considered here – 72, 108, and 215 eV per D – are 0.49, 0.47, and 0.45, respectively. That means that about 50 % of the impinging deuterons do not enter the layer but are kinetically reflected out of the sample surface. It is interesting to note that the corresponding reflection yields for pure W surface are 0.67, 0.65 and 0.62, respectively. That means the presence of N in the surface reduces the reflection yield.

Comparing the D implantation ranges estimated from Fig. 6 with the experimentally determined D depth distribution for D implantation at 300 K (Fig. 5) we find that the thickness of the D-containing layer (about 20 nm) can be solely explained by implantation. It agrees very well with the penetration range of the D species with the highest energy per D stemming from the small fraction of atomic D ions which impinge with the maximum energy of 215 eV. At 600 K, the measured D-containing layer is much thicker (~100 nm) than the calculated implantation ranges. We attribute this to diffusion of implanted deuterons. Therefore, we conclude that at 300 K D implanted into WN_x remains in the implantation zone and does not diffuse into larger depth, while at 600 K D will after thermalization diffuse. Obviously, the onset temperature for D diffusion in WN_x lies between 300 and 600 K. Further experiments for determining this onset temperature are planned. Even though diffusion plays obviously a role on the final D depth

distribution at 600 K, it should be emphasized that for the chosen experimental conditions all the retained D is found within the deposited 135 nm thick WN_x layer and does not reach the underlying W film (as indicated by the W/WN_x interface in Figs. 4&5) substrate. For comparable implantation conditions in bulk, polycrystalline W D would penetrate much deeper and reach depths several micrometers. A direct comparison with D retention in bulk W is difficult, because the latter is strongly dependent on the experimental parameters [22]. For higher implantation energy (200 eV/D) but comparable exposure temperature (573 K) D penetrates more than 6 µm [22]. On the other hand, even at lower implantation energy (38 eV/D) and lower exposure temperature (300 K) D penetrates more than 6 µm [23]. But in both cases the measured D concentrations are significantly lower than in the WN_x films investigated here. It is further interesting to note that D retention in magnetron sputtered films shows a different behavior than in bulk W. A homogeneous filling of magnetron sputtered W films with thicknesses up to 12 µm was reported by Wang et al. (exposure conditions: 38 eV/D, 370 K, D fluence 6×10^{24} Dm^2) [14, 24]. From the comparison of the here measured penetration depth with these literature values we conclude that the diffusivity of D in our WN_x layer is significantly lower than that in bulk or magnetron-sputtered pure W.

4.2 Total retained D amount by NRA

In addition to the implanted D fluence of 1.0×10^{24} D/m^2 presented above a D fluence scan was conducted for the three different sample batches. Fig. 7 shows the total amount of retained D for the three different investigated cases as deduced from the proton counts as described before for a D fluence range between 1.0×10^{23} D/m^2 and 6.0×10^{24} D/m^2. For any investigated D fluence the D amount in as-deposited WN_x exposed at 300 K is always the highest. The pre-annealed samples show a very similar but slightly (10 to 15 %) lower D retention. Samples exposed at 600 K retain only about half of the amount as the 300-K-exposed samples. At 300 K even for the lowest investigated fluence of 1.0×10^{23} D/m^2 the retained D amount corresponds already to 75 % of the retained D amount measured for the 10-times higher fluence. For fluences higher than 1.0×10^{24} D/m^2 the trend is not very clear. The as-deposited sample shows a slight further increase by about 10 %, while the D content in the pre-annealed sample is practically constant in this range. Surprisingly, at low D fluence ($\leq5.0\times10^{23}$ D/m^2), the total retained D amounts from both sets of 300-K-implanted samples first decrease slightly and only then increase with D fluence. Although not easy to understand, this behavior turned out to be reproducible in additional independent experiments. A possible reason for this will be discussed later. The sample exposed at 600 K shows only negligible fluence dependence. The D amount increases by less than 10 % over the whole investigated fluence range. One point worthy to mention is the fraction of the retained D amount compared with the impinging D fluence. Presently, for all 3 sets of samples up to the highest impinging D fluence (6×10^{24} D/m^2), the total retained amount is below 2.5×10^{20} D/m^2. The fraction of retained D

normalized to the incoming D fluence at this highest fluence is roughly 4×10^{-4} at 300 K and 2×10^{-4} at 600 K. Even at the lowest fluence (1×10^{23} D/m^2), the retained fraction is still below 2×10^{-3} at 300 K and roughly 1×10^{-3} at 600 K. The retained fractions are even a factor of 10 or 100 lower than the contribution from the minority ion species D^+ which contributes 1% to the total impinging D flux. In this respect it should also be kept in mind that, as discussed above, about 50 % of the impinging deuterons do not enter the film, but are reflected directly at the surface.

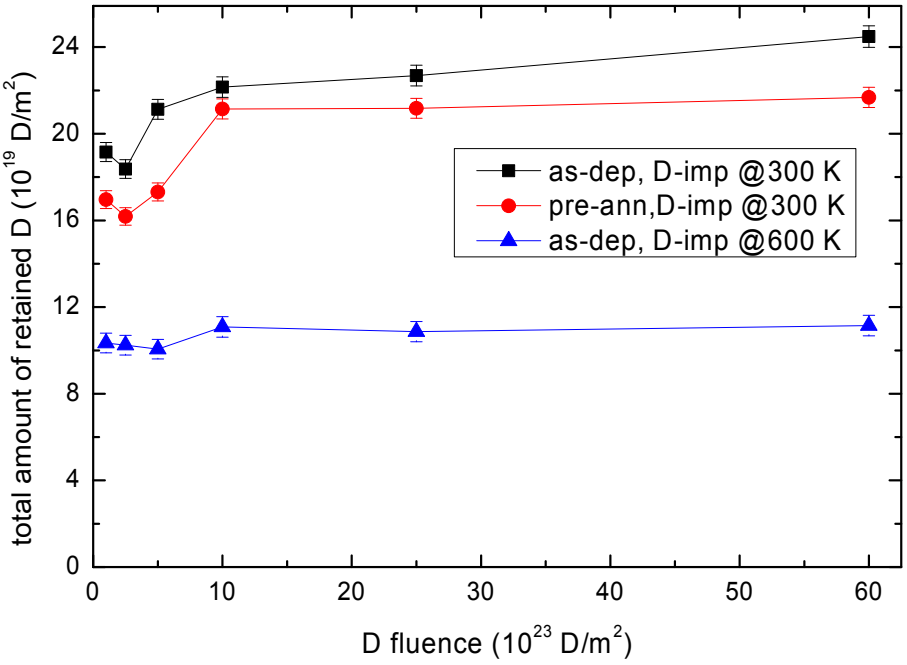

Fig. 7: Total amount of retained D in WN_x samples (measured by NRA) as function of D fluence.

4.3 D release from WN_x: TPD

Samples exposed to the highest D fluence of 6×10^{24} D/m^2 were investigated with TPD measurements. The TPD spectra of D released in form of D_2 (signal mass channel 4) and HD (signal mass channel 3) are shown in Figs. 8a and b, respectively. As one can see in the figure, the release of both D_2 and HD from the samples exposed to D plasma at 300 K sets in at $T \approx 370$ K. In all these cases the release spectrum is composed of 2 release peaks located at about 440 and 520 K. For both species the second peak is lower for the TPD spectrum of the pre-annealed sample. For the sample exposed at 600 K, D_2 release sets in at roughly 500 K and peaks at ~650 K. It is interesting to note that the starting temperature is lower than the

implantation temperature. This is normally not the case for D implantation into pure W [14, 23, 24], where the D release only starts at a temperature very close to the implantation temperature. The N_2 release from these D-exposed WN_x layers was also measured, but it is not plotted in Fig. 8 because of its 2 orders of magnitude higher release rate compared with the D_2 release. Similarly as the reduced WN_x films in Fig. 1, N_2 release in WN_x after D implantation starts only at $T \geq 830$ K when release of D_2 and HD has almost ceased. The released N amount determined from the analysis of the N_2 release peak at 28 amu/q for each of the three samples after D implantation is determined (about 4.7×10^{21} N/m^2) and compared with that prior to D implantation. Unfortunately, the TPD spectrum prior to D implantation was measured using a sample from a different WN_x deposition batch than the TPD spectrum of the sample after D implantation, such that small differences in the N concentration or WN_x layer thickness could lead to small differences in the total N amount. Due to this uncertainty we can at present not make a quantitative comparison. Nevertheless, from the analysis of the N_2 release spectrum we can state that the amount of N released in form of N_2 is comparable to the N amount measured by RBS.

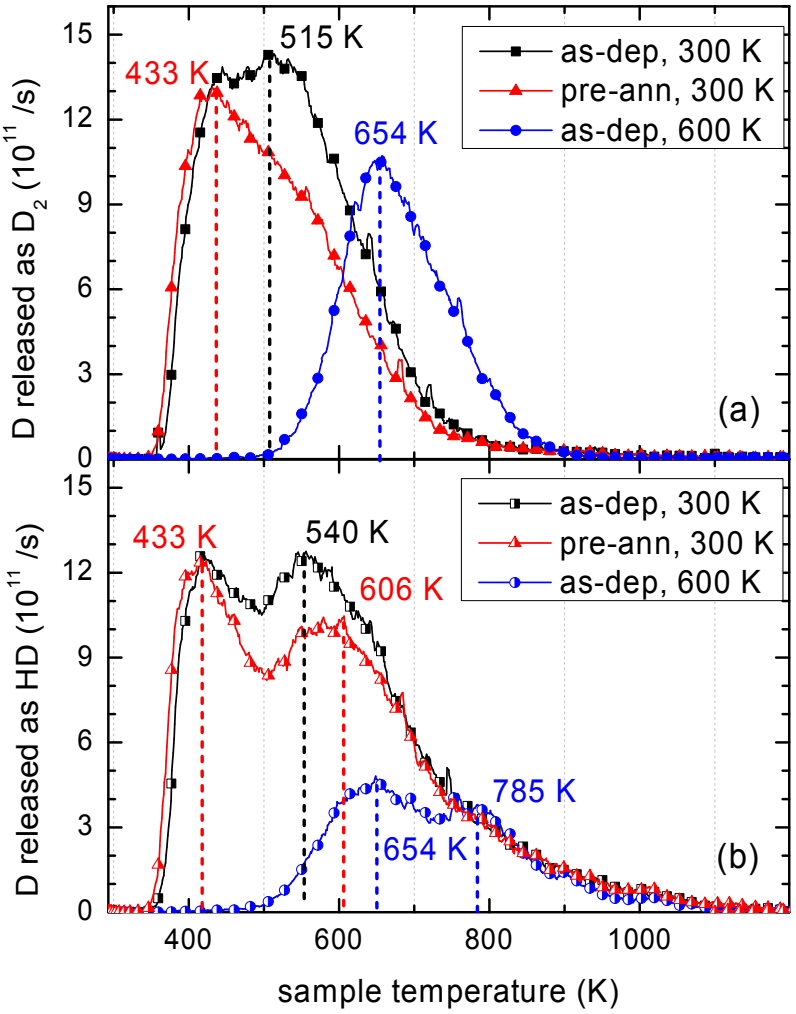

Fig. 8: D release spectra from WN_x samples after exposure with D fluence of 6×10^{24} D/m^2. The peak temperatures of the release spectra are indicated in the figure.

The total D amount released in form of hydrogen molecules (i.e., as D_2 and HD) was determined from the TPD spectra (for calibration see Sect. 2.6) and is listed in Table 1. Surprisingly, in each of the three WN_x samples the amount of D released as molecular hydrogen is roughly a factor of 5 lower than the total retained amount of D measured by NRA. The ratio between TPD and NRA is about 18% and it is almost the same for all the three samples.

Methods \ Samples	as-dep, D6e24@300 K	as-dep, D6e24@600 K	pre-ann, D6e24@300 K
NRA (10^{19} D/m^2)	24.5	11.2	21.7
TPD (10^{19} D/m^2)	4.3	2.1	3.7
TPD/NRA	0.175	0.188	0.171

Table1. Comparison of the retained D amount measured by NRA and the released D amount determined by TPD in WNx samples exposed to a D fluence of 6×10^{24} D/m^2.

Before trying to explain the large difference between the TPD- and NRA-determined D amounts in Tab. 1, it is worth to mention the following information. For pure W samples, NRA depth profiling is normally performed with several different projectile energies up to 4.5 MeV [14, 25] such that the D retention up to a depth of ~8 μm can be determined. It has been demonstrated that the retained D amount measured by NRA and the released D amount by TPD in magnetron-sputtered W films with thickness smaller than this probing depth are in good agreement with each other [14]. For pure W samples with D retained beyond the NRA probing depth, TPD measurements show always a larger amount of released D than the retained D amount by NRA. However, if there are additional loss channels for D retained in the sample that cannot be included in the final D amount calculation from TPD measurements, the NRA-measured amount may also exceed that of TPD. In the experiments described here, the thickness of the D-containing layer in the WN_x films is much smaller than the information depth of the applied NRA measurement. This means NRA measures here the total retained D amount in WN_x. The much lower TPD-measured D amount clearly points to the fact that D is released in form of other gas species than 3 amu/q (HD) and 4 amu/q (D_2).

Although deuterated ammonia isotopologues, such as NH_2D (18), NHD_2 (19) and ND_3 (20), cannot be quantified, we can still compare the release spectra on the corresponding mass channels from the three different D-implanted samples with a not-implanted sample for qualitative understanding, as plotted in Fig. 9. We find significant release peaks on mass channels 18, 19, and 20 amu in the same temperature range where the HD and D_2 release occurs. For these 3 mass channels we find no corresponding release peaks from the WN_x sample that was not implanted with D. From this comparison we conclude that a certain amount of D from the D-implanted samples is released in form of deuterated ammonia and water. Unfortunately, these mass channels cannot be calibrated as discussed in Sect. 2.7. Nevertheless, from the experimental findings that only about 18 % of the retained D is released as molecular hydrogen and that release of deuterated ammonia and water isotopologues is clearly proven by TPD we draw the conclusion that a significant amount – of the order of 80% – of the retained D is released as deuterated ammonia and

water. The apparent contradiction to the finding that no significant amount of N is converted to ammonia is due to the facts that, firstly, the total amount of N in the WN_x layer is about a factor of 23 higher than the D amount (D amount ≈ 2×10^{20} D/m^2 see Fig. 7), secondly, that some D might be released as water and, thirdly, that for the formation of ammonia three hydrogen atoms are required.

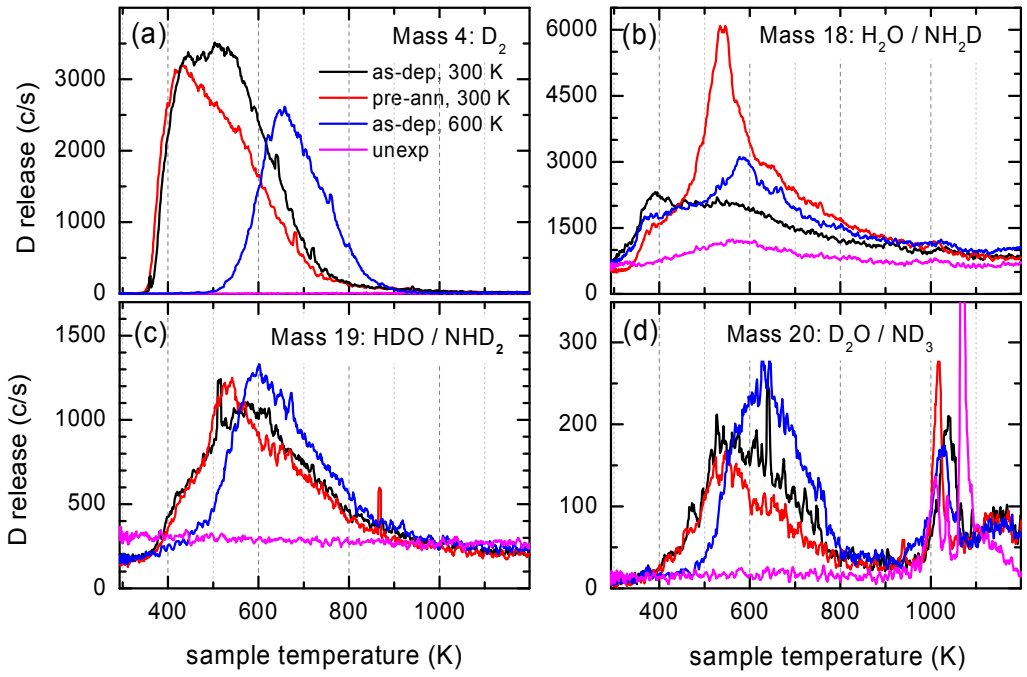

Fig. 9: Comparison of the TPD spectra of different mass channels between WN_x samples exposed to a D fluence of 6×10^{24} D/m^2 (-200 V bias, 300/600 K) and an unexposed WN_x sample: (a) 4 amu/q; (b)18 amu/q; (c)19 amu/q and (d)20 amu/q. No signal of D or deuterated ammonia is found in the unexposed WN_x sample.

5. *WN_x erosion due to D plasma exposure*

5.1 WN_x erosion in D plasma

The erosion of the WN_x layer after D implantation was determined by RBS using a 1.5 MeV $^4He^+$ ion beam. Before discussing the experimental results we would like to make the following comment. The applied substrate bias in the present experiments (-200 V) is not high enough that the dominant D ion species (D_3^+) and also minor species D_2^+ can sputter W. Only the minority species D^+ exhibits an energy that is just above the threshold as to sputter W. However, due to the low fluence of D^+ minority the total sputtered W amount would be too low to be detectable by RBS. Applying the sputter yield for 215 eV D

on W of 2.3×10^{-5} W/D published by Eckstein [26] yields the sputtered tungsten amount for the highest investigated D fluence (6×10^{24} D/m^2) of 1.4×10^{18} W/m^2. This is still less than one monolayer. It should, however, be kept in mind that, although D can under these conditions not sputter pure W it has sufficient energy to sputter N. Because the D species cannot explain the measured W erosion, the sputtering of W from the WN_x layers during the D plasma exposure is attributed to impurity ions contained in the plasma [13].

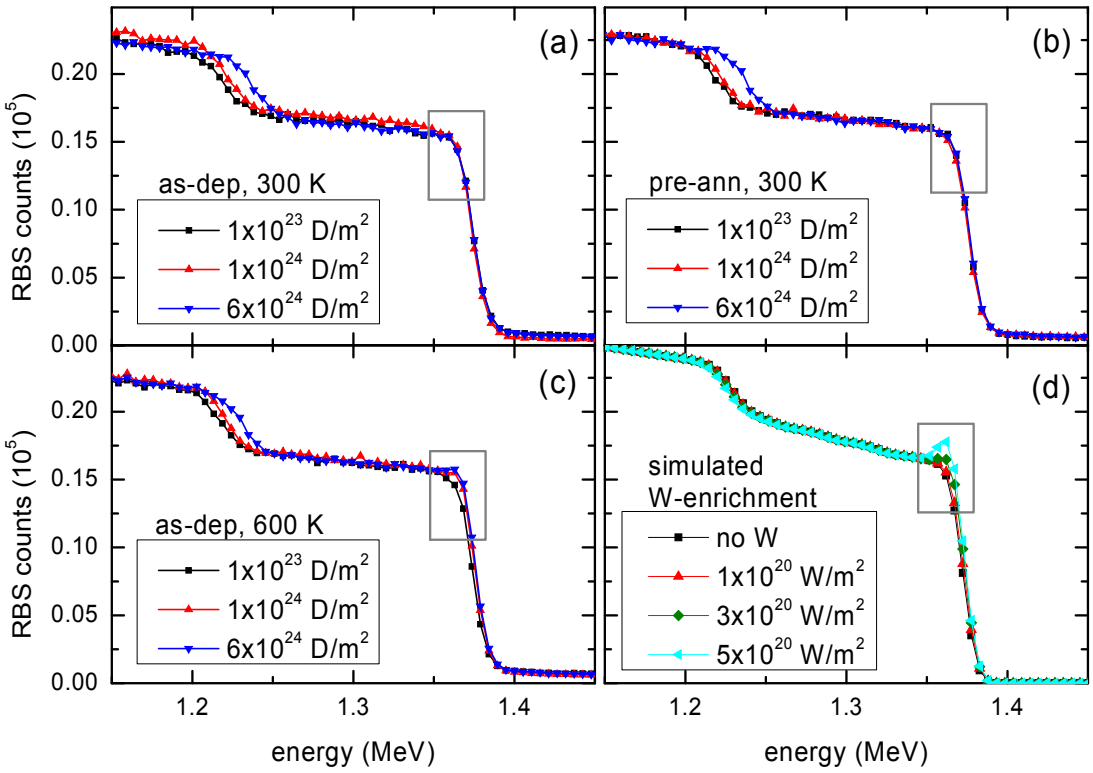

Fig. 10: RBS spectra of magnetron-sputtered WN_x films deposited on 2-µm-W-film-coated-Si substrates after D plasma exposure with different D fluences: a) as-deposited samples exposed at 300 K; b) pre-exposure-annealed samples exposed at 300 K; c) as-deposited samples exposed at 600 K; d) simulated W enrichment with different thicknesses of W layer on top of a WN_x sample.

The shift of the W/WN_x edges at about 1220 keV backscatter energy in the RBS spectra is hardly detectable if the D fluence is lower than 1.0×10^{24} D/m^2. This is the reason why only some selected RBS spectra are shown in each sub-figure of Fig. 10. In sub-figures a-c an obvious shift of the WN_x edge to higher energy is visible after exposure to a D fluence of 6.0×10^{24} D/m^2. The largest shift is found in Fig. 10b for the pre-annealed samples implanted at 300 K. In this case about 16 nm of WN_x were

removed during D loading. At 600 K D implantation temperature only about 9 nm WN_x were eroded after the same fluence.

A detailed comparison of the three sets of RBS spectra shows also a slightly different erosion behavior of WN_x at the two investigated temperatures. For the samples exposed at 600 K (Fig. 10c) the W counts directly at the surface (i.e., at ~ 1370 keV backscattering energy; area marked by the rectangles) show a slight increase as the D fluence increases. A corresponding increase is not found for the samples exposed at 300 K (Fig. 10a, b). To explain this increase of the count rate, SIMNRA simulations were performed, where a thin pure W layer with different thickness was added on top of the WN_x layer. The simulated RBS spectra are shown in Fig. 10d. The simulations are performed such that the total W amount in the whole layer system is kept constant. Nitrogen is removed from a surface layer with increasing thickness. The W from the removed W:N layer is condensed into a pure W layer with the identical total W amount. Fig. 10d illustrates how RBS spectra should evolve if W enrichment (or N depletion) at the surface increases. Comparing Figs. 10c and d suggests that the observed increase in count rate at the surface can be explained by W enrichment at WN_x surfaces exposed to D plasma at 600 K. The W enrichment required to explain the observed changes in the spectra is, however, relatively substantial. It amounts to approximately 3×10^{20} Wm^{-2} which corresponds to roughly 30 monolayers of pure tungsten. For the 300-K exposed WN_x surfaces (Fig. 10a and b), a possible W enrichment is not detectable with RBS. Obviously, at 300 K exposure the W enrichment at the surface is less pronounced than at 600 K such that it cannot be resolved by RBS.

5.2 W enrichment

As just discussed, analysis of the RBS spectra of WN_x surfaces after D implantation suggests a slight enrichment of W at sample surfaces after exposures at 600 K, while at 300 K, no W enrichment is detectable by RBS. To further investigate this issue, WN_x samples were before and after D implantation analyzed by XPS sputter depth profiling. The investigated D-implanted sample was previously exposed to a D fluence of 5×10^{23} D/m^2 at 300 and 600 K. The analysis in the present work focuses on the N 1s peak at ~397 eV and the most intense tungsten peak, W 4f7/2 at ~32 eV. Unfortunately, only few data can be found in the literature on XPS peak shifts for W due to W-nitride formation. The N 1s peak for tungsten nitrides is shifted to lower binding energies compared with molecular nitrogen adsorbed on the W surface, which has a binding energy of about 400.0 eV [27, 28]. The values for N bonded to W reported in the literature vary from 397.0 to 397.7 eV [29-33, 35]. More literature data are available for the W 4f peak. The metallic W 4f7/2 peak exhibits a binding energy of 31.4 eV and the nitrides generally show slightly higher values. Also in this case some scatter in the published data is noticed. Different values for the

binding energy of the W 4f7/2 peak in W nitrides ranging from 31.4 to 33.2 eV were reported in different publications and attributed to different nitride stoichiometries [29-35].

The XPS spectra in the binding energy ranges of these two peaks are shown in Fig. 11. As one can see in Fig. 11a, without D implantation, the here investigated W 4f7/2 peak of the as-deposited layer (squares) is located at 32.4 eV. After D implantation at either temperature, it shifts to lower binding energy (31.4 eV) with roughly 50 % higher intensity at 300 K and even higher intensity at 600 K. According to the published peak positions listed above the latter peak position is the W 4f7/2 peak position of metallic W. Similarly, Fig. 11b shows the change of the N 1s peak after D implantation: the integral of the counts from the N 1s peak decreases by more than 50 % at 300 K and is negligible at 600 K. The binding energy at both temperatures shifts by only 0.2 eV from 397.4 eV to 397.6 eV. Both, the higher W 4f peaks intensity and the lower N 1s intensity point to a higher W concentration in the surface after D implantation at both temperatures.

Although not being resolved in RBS spectra, XPS measurements on sample surfaces exposed to D plasma at 300 K also showed W enrichment. Hence XPS sputter depth profiling was performed on both surfaces exposed to D plasma to a fluence of 5×10^{23} D/m^2 at 300 and 600 K. An unexposed WN_x sample was also measured for comparison. The measured depth profiles are shown in Fig. 12 as a function of Ar fluence. Plotted in this figure are only the W and N fractions (normalized such that W + N = 100%). In the measurement we also find traces of impurities (in particular at the very surface), but these impurities are not considered to be relevant for the further interpretation of the W:N ratio and for sake of clarity they are, therefore, not shown in the figure. The first 2 data points of each depth profile are taken prior to Ar sputtering. They are influenced by the presence of surface adsorbents. Therefore, the W:N ratio of these data points can be influenced by adsorbed nitrogen. The detected impurities are shortly discussed further below. No particular effort was made to reach a reliable quantitative interpretation of the XPS data. Due to impurity adsorption during transport through air and preferential sputtering effects the quantitative interpretation of XPS depth profiles of such WN_x layers is inherently difficult. Nevertheless, a qualitative interpretation of the XPS sputter depth profiles, i.e., the relative differences between the different samples, is possible. And the basic question we want to answer with the XPS depth profiles here is whether or not there is a different W enrichment at the sample surface after D exposure at 300 and 600 K.

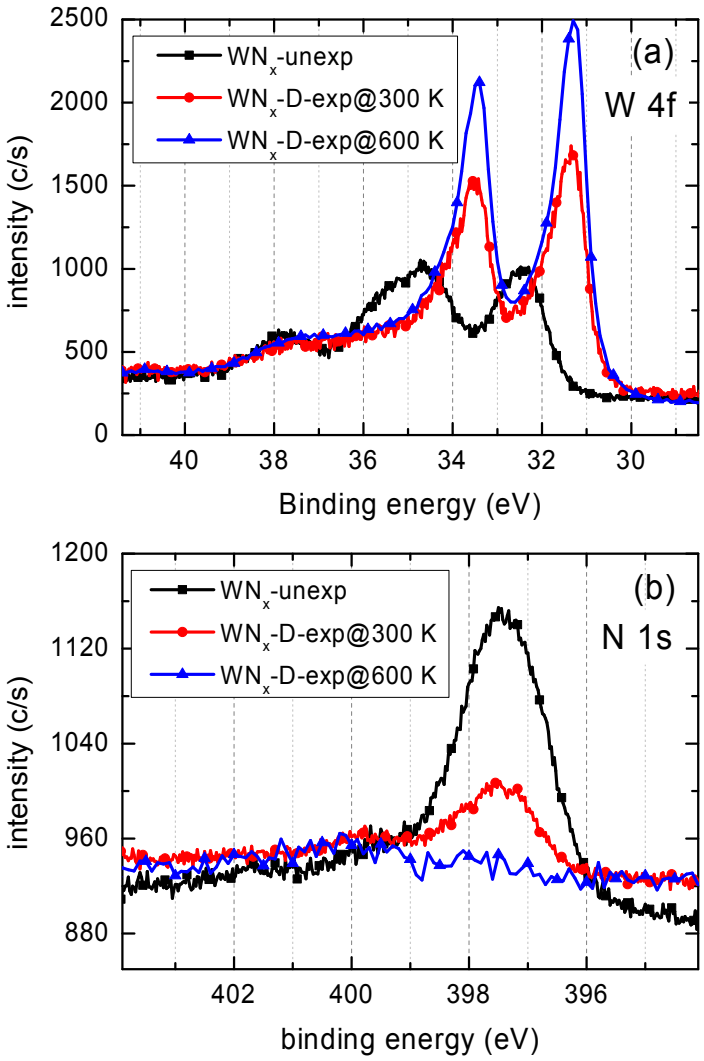

Fig. 11: XPS spectra of WN_x surface before and after exposure to D plasma to a fluence of 5×10^{23} D/m^2. (a) W 4f doublet, (b) N 1s peak. Due to the D plasma exposure, the two W 4f peaks shift to the direction of metallic W 4f. In addition, the N 1s peak intensity decreases significantly.

The as-deposited (i.e., unexposed) sample shows initially a slight increase of the W and a corresponding decrease of the N fraction. This transient change in surface composition is assumed to be due to preferential sputtering of N during Ar sputter depth profiling. It seems that after about half of the measurement the surface concentrations reach a steady state value with a W:N ratio of about 75:25. Surprisingly, the initial W:N ratio of about 65:35 is significantly higher than the W:N ratio determined by RBS (56:44, see Sect. 3). The reason for that is not fully clear, but it is attributed to uncertainties in the

evaluation of the XPS data. The fact that the steady-state W:N ratio of about 75:25 differs from the initial value is attributed to preferential sputtering. During sputtering with Ar, nitrogen is preferentially eroded from the surface such that the W fraction within the XPS information depth (about 3 to 5 nm) is increased.

The sample exposed to D plasma at 300 K shows a significantly higher W surface concentration than the unexposed sample. This is in agreement with the anticipated removal of N from the surface due to D implantation (see also in Fig. 11). After an Ar fluence of about 20 to 30×10^{19} Ar/m^2 the W:N ratio approaches the values measured for the unexposed sample. The remaining difference between the unexposed and 300-K-exposed samples is attributed to uncertainties in the XPS evaluation.

The sample exposed to D plasma at 600 K has a much higher W surface concentration and this higher W concentration extends to a much larger depth than for the 300-K case. The N content close to the surface is almost zero and it starts to increase for Ar fluences larger than about 4×10^{19} Ar/m^2. The required Ar fluence to reach a quasi-steady-state is about 10×10^{19} Ar/m^2. This is about 3 times more than for the 300-K-exposed sample. Towards the end of the measurement all 3 samples seem to approach a common steady-state value. This behavior is anticipated because after removal of the surface layer modified by the D plasma exposure the underlying WN_x layers are more or less identical. In spite of the remaining uncertainties in the absolute W:N ratios we can state that from XPS sputter depth profiling a clear W enrichment at the surface was found and that the thickness of this W-enriched layer is about a factor 3 larger for the sample exposed at 600 K as compared with the sample exposed at 300 K.

The total sputter crater depth after argon sputtering was not measured, but assuming that the rate determining step is sputtering of W by Ar we can estimate the removed W amount. The sputter yield for 10 keV Ar on W is about 2.3 [26]. That means that after the longest applied Ar fluence of 1.5×10^{20} Ar/m^2 about 3.4×10^{20} W/m^2 were removed. This corresponds to the W amount in an approximately 8.5 nm thick layer of our WN_x film (for comparison: the thickness of a corresponding bulk tungsten layer would be 5.4 nm). Taking this value as a rough estimate for the sputter depth scale, we arrive at the following numbers. The depth to reach a steady-state value of the W:N ratio in the unexposed sample due to preferential sputtering of N by Ar is about 4.0 nm. The found W enrichment for the 300-K-exposed sample corresponds to about 1.5 to 2.0 nm and for the 600-K-exposed sample 5.0 to 6.0 nm. This observation is in agreement with the RBS results presented in Sect. 5.1 which also indicated a stronger W enrichment for the sample exposed to D at 600 K. The reason for this stronger N removal at 600 K is presently not known. A possible explanation is that the removal of N by D is more efficient at higher temperature due to an enhanced diffusion or chemical reactivity.

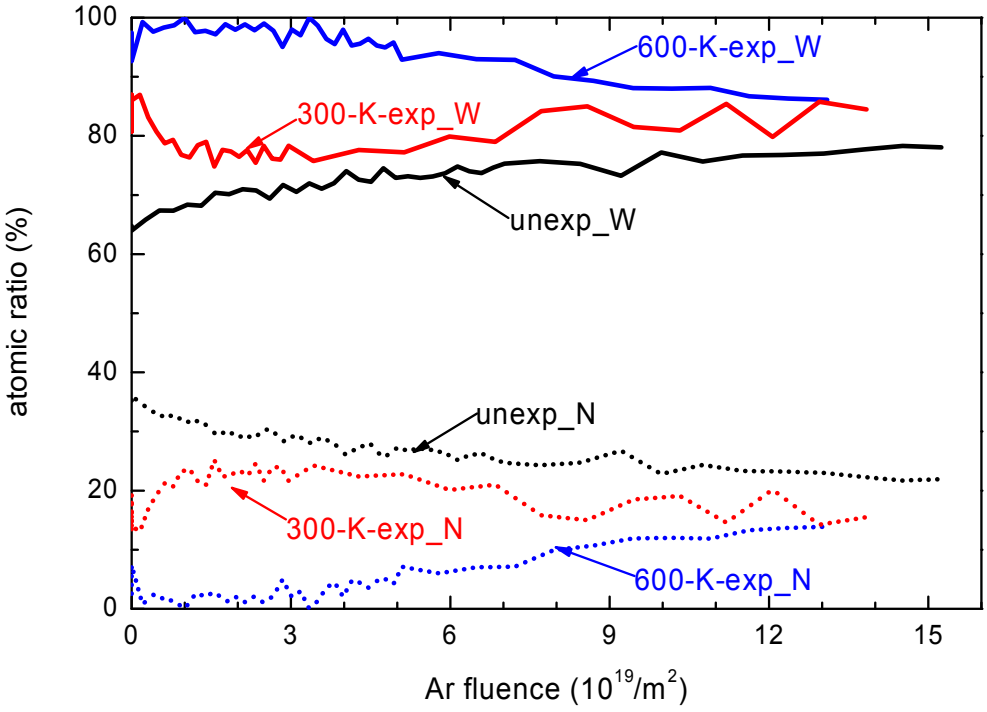

Fig. 12: Ar-sputter XPS depth profiles of unexposed WN_x and WN_x after exposure to D plasma to a fluence of 5×10^{23} D/m^{23} at 300 and 600 K.

5.3 N content

XPS measurements show the removal of N from the surface after D plasma exposure. To determine how much N in WN_x is removed by D, the remaining N amount in WN_x layers after D plasma exposure was extracted from the simulation of the RBS spectra as described before (see in Sec. 2.5). The nitrogen areal densities measured by RBS are plotted as a function of D fluence in Fig. 13. The initial N content prior to D exposure is for all samples identical within the experimental uncertainty. This also proves that the pre-exposure annealing at 600 K does not change the N content, i.e., no desorption of N from the WN_x layers occurs at 600 K for the here deposited WN_x layers. In general, the N amount decreases with increasing D fluence for all the three groups of samples. The decrease is almost identical for all 3 sets of samples. It seems to be slightly higher for the as-deposited samples with D implantation at 300 K. The total decrease of the N content after the maximum fluence of 6×10^{24} D/m^2 correspond to about 18 %.

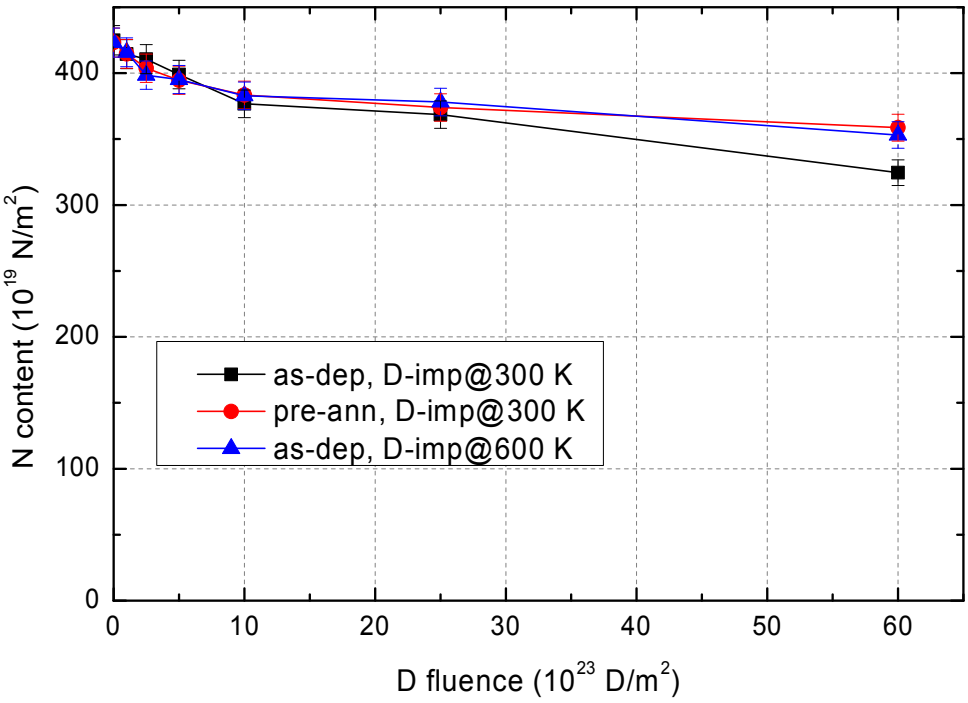

Fig. 13: Amount of N in WN_x samples as function of D fluence as deduced from the shift of the RBS tungsten edge and height. The decrease of N in the WN_x layer is in general rather small.

6. Discussion

6.1 D in WN_x

The new analysis method presented in Sect. 2.5 comprising low-energy Ar plasma sputtering combined with NRA analysis of D retention is capable of resolving the D depth profile at the surface with a depth resolution of less than 3 nm which is superior to the standard NRA depth resolution (16 nm in our set-up for the analysis of the alpha particles from the nuclear reaction, see [14, 25]). This allows resolving the implantation depth profile of low-energy (215 eV) D implanted into WN_x layers.

D implanted at 300 K into WN_x layers is found in a near surface layer with a thickness of about 19 nm. Comparison with SDTrimSP simulation results (Figs. 5 and 6) yields that this thickness corresponds to the implantation depth of the small fraction of atomic D^+ ions which impinge with the full energy of 215 eV. The molecular ions, D_3^+ and D_2^+, have a lower energy per deuteron and correspondingly a smaller penetration depth. From this good agreement we draw the conclusion that at

300 K the implanted D does not diffuse, but stays where it is implanted. The retained D amounts are of the order of 2×10^{20} D/m^2 (Fig. 7). The fraction of impinging D that is retained is very low. Even for the lowest investigated fluence of 1×10^{23} D/m^2 only a fraction of 10^{-3} of the impinging deuterons is retained. In this context it should, however, be kept in mind that the reflection yield calculated with SDTrimSP for the conditions of this experiment is 0.49 for the majority ions. The saturation of the retained amount sets in at a fluence of about 1×10^{24} D/m^2. That also means that most of the implanted deuterons must diffuse back to the surface and desorb. We assume that within the ion penetration range D can diffuse due to ion-impact-induced diffusion.

At 600 K the D depth profile is significantly broader than that at 300 K. The total retained D and the local D concentrations are lower, but the penetration depth is much larger than the implantation range. This is a clear proof that at 600 K D diffuses into larger depth. Comparing the penetration in WN_x layers with that in pure W [14, 15, 22-24] we find that the range for WN_x is much lower than for W. That means that the diffusion coefficient of D in WN_x is much lower than that in bulk W. In addition, the D concentration in the WN_x layer is much higher than in pure W (about 14 at.% at 300 K). The maximum D concentration is found almost at the end of the implantation range of the D species with the highest energy (the D^+ ions impinging with 215 eV, see Fig. 6). For D implantation at 600 K the peak concentration is about 3%. The total retained D amount at 600 K is only about half of that at 300 K. To check whether the reduced D retention at 600 K is due to a change of the microstructure or due to the higher implantation temperature, one sample was first annealed at 600 K for 2 h and then exposed to D plasma at 300 K. This sample shows about 10 % lower D retention than the sample that was not pre-annealed (see Fig. 7). From this we conclude that the pre-annealing does not lead to a significant change of the retention capability and that, therefore, the lower total retention at 600 K is due to the higher implantation temperature. The slightly lower retained D amount in pre-annealed samples compared with as-deposited samples may be due to the fact that the pre-exposure annealing moderately annihilated some trapping sites inside the WN_x layer. Such a minor change could also explain the small increase of the decomposition temperature of the layer after annealing as presented in Fig. 1. Based on the observation that the pre-annealed sample shows only a 10 % lower D retention we conclude that the lower local D concentration at 600 K is not governed by the annealing of possible trap sites, but is dominantly attributed to thermal detrapping during D exposure which leads to a lower occupation of available trap sites. The fact that thermal detrapping is active at these temperatures is clearly shown in the TPD spectra of Figs. 8 and 9.

The D concentration in WN_x exposed to D plasma at 600 K is significantly higher than in pure W materials in the region beyond the implantation depth. The mean D concentration in WN_x in the range

from about 15 to 50 nm is roughly 1%. For similar loading conditions the D concentration in pure W materials is typically of the order of 10^{-3} for the depth range from about 16 nm up to a few μm [14, 15, 23, 24] at 300 K and much lower at 600 K (10^{-4}) [23]. Magnetron-sputtered W films normally exhibit 3-4 times higher D concentration than that in warm-rolled polycrystalline W [14, 15, 24]. The D concentration in our WN_x layers is about a factor of 4 higher than that in magnetron-sputtered W films. We suggest that N in the W matrix acts as a trap site for D thus significantly enhancing D retention in comparison with pure W. Noteworthy is the stable bonding of the D retained in the WN_x layers. It was observed for pure W that up to 30% of the retained D is lost from the sample after storage for 2 months. However, this is not the case for our WN_x samples. NRA measurements performed on these samples at different times after exposure, namely 1 day, 3 weeks and 3 months after D implantation, showed within the experimental uncertainty the identical D amount. This means there is almost no loss of D in WN_x layers during storage.

Intriguing is the decrease of the total retained D amount with increasing D fluence at low fluence (below 1×10^{24} D/m^2, see Fig. 7) in both samples exposed at 300 K. As mentioned in Sect. 3.2 this behavior is reproducible. Since D does not diffuse in WN_x at 300 K, the final retained D amount in WN_x at 300 K depends strongly on the amount of D trap sites within the implantation zone. In the preceding paragraph we speculated that the D retention in WN_x is governed by bonding to N. At very low D fluence N is abundant at the top-most surface and we assume that initially the retained D amount increases linearly with D fluence. But, as the D fluence increases more and more N will be removed from the implantation region. It is conceivable that a certain fraction of the initially retained D is released together with the N thus leading to a decrease of the retained D amount with increasing D fluence. At a certain D fluence, probably when most of the N is removed from the implantation zone, the total retained D will decrease to a minimum. After that transition period the total retained D amount again starts to increase slowly with D fluence. For D implantation into WN_x at 600 K, the thermal detrapping and also the diffusion of the implanted D come into play. Therefore, the decrease at low D fluence is much less pronounced as that at 300 K. It is, unfortunately, not feasible to investigate lower D fluences in PlaQ due to the relatively high ion flux. Further experiments in another device with much lower ion flux are planned in the near future.

6.2 Formation of ammonia

As a speculation, we attribute the decrease of the N amount in WN_x layer with increasing D fluence at least partially to the formation of ammonia. Unfortunately, the amount of ammonia during plasma exposure cannot be measured under the present conditions. On the one hand, the production of ammonia

is very low. Up to a D fluence of 6.0×10^{24} D/m^2, the reduction of N amount in the layer is less than 15%. As shown above, during D implantation, the surface will be enriched with W due to the removal of N. This very thin W layer will reduce the further N loss by suppressing the out-diffusion of formed ammonia in the subsurface. On the other hand, ammonia itself will strongly stick to the chamber wall, which makes the detection even more difficult. Therefore, comparing the N content in the surface before and after D exposure is the only possible way to assess the formation of ammonia during D implantation under the present conditions. The amount of lost N provides an upper limit on the evaluation of ammonia formation. The presented TPD measurements have shown clear evidence for the formation of ammonia after D implantation into WN_x layers. Although the amount of ammonia cannot be quantified under the present experimental conditions, we found that only about 18 % of the retained D is released as molecular hydrogen. Assuming that no D is retained in the layer after the end of the TPD analysis (we could not test this assumption because the layers delaminated completely after TPD) up to about 80 % of the originally retained D could be released as water or ammonia. Since the oxygen content of our samples is negligible compared to the nitrogen content it is reasonable to assume that most of this D is released as ammonia. Release of ammonia occurs together with the release of molecular hydrogen at relatively low temperatures ($\leq$ 650 K).

7. Summary

The interaction of D plasma with sputter-deposited WN_x layer was studied at two temperatures, 300 and 600 K. TPD measurements have shown that the sputter-deposited WN_x layers are thermally stable up to about 800 K. Decomposition starts at around 830 K with two release peaks at 925 and 960 K. A new D depth profiling method consisting of low-energy Ar sputtering combined with NRA analysis of the remaining D amount shows great potential in resolving D depth distribution with a few nanometers resolution. The new method allowed the determination of D depth profiles by NRA with unprecedented depth resolution of 3 nm. Results show that at 300 K the implanted D is retained only within the implantation zone. At 600 K D diffuses to larger depth, but the diffusivity of D in WN_x is substantially lower than in pure W. It appears that WN_x acts as a diffusion barrier for diffusion of D in W, but further investigations are necessary to support this assumption. The local concentration of D retained in WN_x beyond the implantation zone after exposure at 600 K is relatively high. It is about a factor of 10 higher than in standard polycrystalline tungsten and a factor of 3 higher than in sputter-deposited pure W films exposed at 300 K. This relatively high local D concentration is attributed to the presence of N which is suggested to act as a trap for hydrogen isotopes. Results from both RBS and XPS measurements show different processes on the WN_x surfaces exposed at different temperatures. The W enrichment and N removal are less pronounced at 300 K than at 600 K. D is thermally released from WN_x in the temperature

range from 400 to 700 K. Surprisingly, only about 18% of the retained D is released as hydrogen molecules. Based on the available data it was concluded that up to 80 % of the retained D is released as deuterated ammonia or water. At present, these two species cannot be surely distinguished, but it is assumed that ammonia isotopologues dominate. The release of ammonia occurs together with the release of molecular hydrogen.

Acknowledgements

This work has been carried out within the framework of the EUROfusion Consortium and has received funding from the Euratom research and training programme 2014-2018 under grant agreement No 633053. The views and opinions expressed herein do not necessarily reflect those of the European Commission.The work was partially carried out under WP PFC. The stay of L. Gao at Max-Planck Institute für Plasmaphysik in Garching was partially funded through a Joint Doctoral Promotion Programme between Max-Planck Society and the Chinese Academy of Sciences, which is gratefully acknowledged. Intense discussions with Dr. Klaus Schmid and Dr. Matej Mayer on the interpretation of experimental results are highly appreciated. Thanks are further due to Michael Fußeder and Joachim Dorner for their help with ion beam measurements, and to Stefan Elgeti for his help on FIB cutting.

References:

[1] Roth J., Tsitrone E., Loarer T. *et al.* 2008 *Plasma Phys. Contr. Fusion* **50** 103001

[2] Neu R., Kallenbach A., Balden M. *et al.* 2013 *J. Nucl. Mater.* **438, Supplement** S34

[3] Neu R. L., Brezinsek S., Beurskens M. *et al.* 2014*, IEEE Trans. Plasma Sci.* **42** 552

[4] Kallenbach A., Dux R., Fuchs J. C. *et al.* 2010 *Plasma Phys. Contr. F.* **52** 055002

[5] Kallenbach A., Bernert M., Eich T. *et al.* 2012 *Nucl. Fusion* **52** 122003

[6] Zagorski R., Neu R. and ASDEX Upgrade Team. 2012 *Contrib. Plasm. Phys.* **52** 379

[7] Oberkofler M., Douai D., Brezinsek S. *et al.* 2013 *J. Nucl. Mater.* **438, Supplement** S258

[8] Brezinsek S and JET-EFDA contributors. 2015 *J. Nucl. Mater.* **463** 11

[9] Rubel M., Philipps V., Marot L. *et al.* 2011 *J. Nucl. Mater.* **415** S223

[10] Gao L., Jacob W., Wang P. *et al.* 2014 *Phys. Scripta* **2014** 014023

[11] Lee H. T., Ishida M., Ohtsuka Y. *et al.* 2014 *Phys. Scripta* **2014** 014021

[12] Gao L., Jacob W., Schwarz-Selinger T. *et al.* 2014 *J. Nucl. Mater.* **451** 352

[13] Gao L. unpublished results. Max-Planck-Institut für Plasmaphysik (Garching)

[14] Wang P., Jacob W., Gao L. *et al*. 2013 *Nucl. Instr. Meth. Phys. B* **300** 54

[15] Wang P., Jacob W., Gao L. *et al*. 2014 *Phys. Scripta* **2014** 014046

[16] Salançon E., Dürbeck T., Schwarz-Selinger T. *et al*. 2011, *J. Nucl. Mater*. **376** 160

[17] Manhard A., Schwarz-Selinger T. and Jacob W. 2011 *Plasma Sources Sci. T.* **20** 015010 ***Note:*** *Unfortunately, the information given in the last paragraph of this article is not correct, but the information in figures 5 and 6 is correct. The contribution of the molecular ions to the total ion flux for standard conditions is: D_3^+ = 94%, D_2^+ = 3% and D^+ = 3%. Correspondingly, the contributions to the total deuteron flux in form of ions are: 97%, 2%, and 1%.*

[18] Alimov V. K., Mayer M. and Roth J. 2005 *Nucl. Instr. Meth. Phys. B* **234** 169

[19] Mayer M. "SIMNRA user's guide" 1997 *IPP Report*: **IPP 9/113**

[20] Möller W., Eckstein W. and Biersack J. P. 1988 *Comput. Phys. Commun*. **51** 355

[21] Mutzke A., Schneider R., Eckstein W. and Dohmen R., 2011 *IPP Report* **12/08**, MaxPlanck-Institut für Plasmaphysik (Hrsg.) (http://edoc.mpg.de/display.epl?mode=doc&id=552734)

[22] Roth J. and Schmid K. 2011 *Phys. Scripta* **T145** 014031

[23] Manhard A., Schmid K., Balden M. *et al*. 2011 *J. Nucl. Mater*. **415** S632

[24] Wang P., Jacob W. and Elgeti S. 2015 *J. Nucl. Mater*. **456** 192

[25] Schmid K. and von Toussaint U. 2012 *Nucl. Instr. Meth. Phys. B* **281** 64

[26] W. Eckstein in Topics in Applied Physics Vol. **110** "Sputtering by Particle Bombardment IV", Springer Verlag, Berlin, 2007, R. Behrisch and W. Eckstein (Eds.), chapter "Sputtering Yields", pages 33-187

[27] Fuggle J. C. and Menzel D. 1979 *Surf. Sci.* **79** 1

[28] Egawa C., Naito S. and Tamaru K. 1983 Surf. Sci. **131** 49

[29] Nakajima T., Watanabe K. and Watanabe N. 1987 J. Electrochem. Soc. **134** 3175

[30] Lee Ch.-W., Kim Y.T. and Min S.-K. 1993 Appl. Phys. Lett. **62** 3312

[31] Kakanakova-Georgieva A., Kassamakova L., Marinova Ts., 1999Appl. Surf. Sci. **151** 225

[32] Shen Y.G., Mai Y.W., McKenzie D.R. *et al.* 2000 J. Appl. Phys. **88** 1380

[33] Baker C.C. and Shah S.I. 2002J. Vac. Sci. Technol. A **20** 1699

[34] Schmid K., Manhard A., Linsmeier C. *et al.* 2010 *Nucl. Fusion* **50** 025006

[35] Meisl G., Schmid K., Encke O. *et al.* 2014 *New Journal of Physics* **16** 093018